IEM-FT-168/98
hep–ph/9801272

# Bubbles in the Supersymmetric Standard Model *

**J.M. Moreno, M. Quirós and M. Seco**

Instituto de Estructura de la Materia, CSIC, Serrano 123, 28006-Madrid, Spain



**Abstract**

We compute the tunneling probability from the symmetric phase to the true vacuum, in the first order electroweak phase transition of the MSSM, and the corresponding Higgs profiles along the bubble wall. We use the resummed two-loop temperature-dependent effective potential, and pay particular attention to the light stop scenario, where the phase transition can be sufficiently strongly first order not to wipe off any previously generated baryon asymmetry. We compute the bubble parameters which are relevant for the baryogenesis mechanism: the wall thickness and $\Delta\beta$. The two-loop corrections provide important enhancement effects, with respect to the one-loop results, in the amount of baryon asymmetry.

IEM-FT-168/98
January 1998

*Work supported in part by the European Union (contract CHRX/CT92-0004) and CICYT of Spain (contract AEN95-0195).

# 1 Introduction

Electroweak baryogenesis [1] is an appealing mechanism to explain the observed value of the baryon-to-entropy ratio, $n_B/s \sim 10^{-10}$, at the electroweak phase transition [2, 3], that can be tested at present and future high-energy colliders. Although the Standard Model contains all the necessary ingredients [1] for a successful baryogenesis, it fails in providing enough baryon asymmetry. In particular it has been proven by perturbative [4, 5, 6] and non-perturbative [7] methods that, for Higgs masses allowed by present LEP bounds, the phase transition is too weakly first order, and any previously generated baryon asymmetry would be washed out after the phase transition. On the other hand the amount of CP violation arising from the CKM phase is too small for generating the observed baryon asymmetry [8]. Therefore electroweak baryogenesis requires physics beyond the Standard Model at the weak scale.

Among the possible extensions of the Standard Model at the weak scale, its minimal supersymmetric extension (MSSM) is the best motivated one. It provides a technical solution to the hierarchy problem and has its roots in more fundamental theories unifying gravity with the rest of interactions. The MSSM has new violating phases [9] that can drive enough amount of baryon asymmetry [10]-[16] provided that the previous phases are not much less than 1 and the charginos and neutralinos are not heavier than 200 GeV [1]. As for the strength of the phase transition [17]-[19], a region in the space of supersymmetric parameters has been found [20]-[28] where the phase transition is strong enough to let sphaleron interactions go out of equilibrium after the phase transition and not erase the generated baryon asymmetry. This region (the so-called light stop scenario) provides values of the lightest Higgs and stop eigenstates which are: 75 GeV $\lesssim m_h \lesssim$ 105 GeV, 100 GeV$\lesssim m_{\tilde{t}} \lesssim m_t$. It will be covered at LEP2 and Tevatron colliders.

In all calculations of the baryon asymmetry the details of the wall parameters play a prominent role in the final result. In particular the wall thickness, $L_\omega$, and the relative variation of the two Higgs fields along the wall, $\Delta\beta$, are typical parameters which the generated baryon asymmetry depends upon. Although reasonable assumptions about the Higgs profiles along the wall have been done, as e.g. kinks or sinusoidal patterns interpolating between the broken and the symmetric phases, as well as estimates on the value of $\Delta\beta$ based on purely potential energy considerations, it is clear that the reliability of those estimates as well as more precise computations of the baryon asymmetry

[1] The first and second generation squarks are required to have masses $\mathcal{O}$(few) TeV because of the experimental bounds on the neutron electric dilope moment.

should rely on realistic calculations of the Higgs profiles and the tunneling processes from the false to the true vacuum. Such a task, having been achieved in the case of one Higgs field in the Standard Model [29], was still missing in the case of two-Higgs field models.

In this paper we compute the tunneling probability from the false to the true vacuum in the first order electroweak phase transition of the MSSM, and the corresponding Higgs profiles along the wall. In particular we will concentrate in the region of the supersymmetric parameters corresponding to the light stop scenario, where the phase transition is strong enough not to wash out the generated baryon asymmetry. We will use the MSSM effective potential at finite temperature including the most important two-loop corrections. The two-loop corrections have been proven to be very important in determining the strength of the phase transition and we will demonstrate that they also play a very relevant role in the baryogenesis mechanism. In particular we will compare the results using the one-loop effective potential, that has been used so far for the determination of the baryon asymmetry, with the corresponding two-loop results. We will see that there is an important enhancement coming from two-loop effects. The plan of the paper is as follows. In section 2 the method to compute the bubbles in the MSSM will be described in detail. The results of our numerical analysis will be presented in section 3. The possibility of bubbles involving squark fields will be explored in section 4 and section 5 is devoted to draw our conclusions.

# 2 Higgs Bubbles

The Higgs sector of the MSSM requires two Higgs doublets, with opposite hypercharges, as

$$H_1 = \begin{pmatrix} H_1^0 \\ H_1^- \end{pmatrix}_{-1/2} \quad ; \qquad H_2 = \begin{pmatrix} H_2^+ \\ H_2^0 \end{pmatrix}_{1/2} \tag{2.1}$$

and tree-level potential:

$$\begin{aligned} V^{(0)} &= m_1^2 H_1^\dagger H_1 + m_2^2 H_2^\dagger H_2 + m_3^2 (H_1 H_2 + h.c.) \\ &\quad + \frac{1}{8} g^2 \left( H_2^\dagger \vec{\sigma} H_2 + H_1^\dagger \vec{\sigma} H_1 \right)^2 + \frac{1}{8} g'^2 \left( H_2^\dagger H_2 - H_1^\dagger H_1 \right)^2 \end{aligned} \tag{2.2}$$

The field configuration describing the tunneling in a theory with just one scalar field in three or more dimensions is known to be spherically symmetric [30]. Here we will assume that the bubbles driving the electroweak phase transition in the MSSM and involving the two neutral higgses also have spherical symmetry. They correspond to the

ansatz:

$$H_1(\vec{x}) = h_1(r) \begin{bmatrix} 1 \\ 0 \end{bmatrix} \; ; \qquad H_2(\vec{x}) = h_2(r) \begin{bmatrix} 0 \\ 1 \end{bmatrix} \, , \tag{2.3}$$

where $r \equiv \sqrt{\vec{x}^{\,2}}$. In the presence of the background (2.3) the tree-level potential reads as

$$V^{(0)}(h_1, h_2) = m_1^2 \, h_1^2(r) + m_2^2 \, h_2^2(r) + 2 \, m_3^2 h_1(r) h_2(r) + \frac{g^2 + g'^2}{8} \left[ h_1^2(r) - h_2^2(r) \right]^2 \tag{2.4}$$

and the one-loop corrections, in the 't Hooft-Landau gauge and in the $\overline{\rm MS}$ renormalization scheme, are given by

$$V^{(1)}(h_1, h_2) = \sum_i \frac{n_i}{64\pi^2} m_i^4(h_1, h_2) \left[ \log \frac{m_i^2(h_1, h_2)}{Q^2} - C_i \right] \tag{2.5}$$

where $Q$ is the $\overline{\rm MS}$ renormalization scale, $C_i$=3/2 (5/6) for scalar bosons and fermions (for gauge bosons), $m_i^2(h_1, h_2)$ is the field dependent mass of the $i^{\rm th}$ particle in the background $h_1$, $h_2$, and $n_i$ is the corresponding number of degrees of freedom, which is taken negative for fermions.

By minimizing the effective potential $V^{(0)} + V^{(1)}$ with respect to $(h_1, h_2)$, and imposing the minimum of the potential to be at $(v_1, v_2)$, with $v = \sqrt{v_1^2 + v_2^2} = 174.1$ GeV, and $\tan\beta = v_2/v_1$ fixed, we can eliminate $m_1^2$ and $m_2^2$ in favour of the other parameters of the theory, while $m_3^2$ can be traded in favour of the one-loop corrected squared mass $m_A^2$ of the CP-odd neutral Higgs boson [19].

Then we can write the finite temperature effective potential as

$$V(h_1, h_2, T) = V^{(0)}(h_1, h_2) + V^{(1)}(h_1, h_2) + \Delta V(h_1, h_2, T) \tag{2.6}$$

where the thermal correction $\Delta V$ contains the one-loop [19], $\Delta V^{(1)}(h_1, h_2, T)$, plus the leading two-loop radiative corrections [25, 26, 28], $\Delta V^{(2)}(h_1, h_2, T)$, of the daisy resummed theory. Since the two-loop corrections have been proved to be very relevant for the strength of the phase transition [25], and present estimates of bubble parameters are based on one-loop thermal corrections, we will often compare our numerical two-loop calculations of these parameters with one-loop results.

The Euclidean action of configuration (2.3) is given by:

$$S_3(T) = 4\pi \int dr \; r^2 \left[ \left( \frac{d\, h_1}{d\, r} \right)^2 + \left( \frac{d\, h_2}{d\, r} \right)^2 + V(h_1, h_2, T) \right] \tag{2.7}$$

where $V(h_1, h_2, T)$ is the effective potential given in (2.6), shifted in such a way that

$V(0,0,T) = 0$. The bubble is then the solution of the equations

$$\begin{aligned} \frac{d^2h_1}{dr^2} + \frac{2}{r}\frac{dh_1}{dr} &= \frac{1}{2}\frac{\partial V}{\partial h_1} \\ \frac{d^2h_2}{dr^2} + \frac{2}{r}\frac{dh_2}{dr} &= \frac{1}{2}\frac{\partial V}{\partial h_2} \end{aligned} \tag{2.8}$$

supplied by the boundary conditions

$$\left.\frac{dh_i}{dr}\right|_{r=0} = 0; \qquad h_i|_{r=\infty} = 0 \qquad (i = 1, 2)\ . \tag{2.9}$$

This solution only exists in the range $T_d < T < T_0$, where $T_d$ is the temperature at which the minimum at $(h_1, h_2)$ is degenerate with that at the origin, and $T_0$ is the temperature at which the origin gets destabilized along some direction and becomes a saddle point.

Solving the previous differential equations is a difficult task. There is no systematic procedure to find the solution. For example, the usual overshooting-undershooting method cannot be implemented in the two (or more) field case. A possible technique is to define a functional, acting in some space, having its minimum at the solution of the previous equations. Notice that the bubble solution is a saddle point of the Euclidean action, *not* a minimum, so we cannot use directly $S_3$. One possibility, explored in reference [31], is to add to $S_3$ some (nonlocal) terms that lift the falling directions. Then the bubble is a minimum of this *improved* action. Here we will follow a slightly different approach. We will consider the following functional [2]

$$\mathcal{F} = 4\pi \int dr\ r^2 \left[ \left( \frac{d^2h_1}{dr^2} + \frac{2}{r}\frac{dh_1}{dr} - \frac{1}{2}\frac{\partial V}{\partial h_1} \right)^2 + \left( \frac{d^2h_2}{dr^2} + \frac{2}{r}\frac{dh_2}{dr} - \frac{1}{2}\frac{\partial V}{\partial h_2} \right)^2 \right] \tag{2.10}$$

By construction, the bubble solution is a minimum of the functional $\mathcal{F}$. In order to find numerically this solution, we have discretized the radial integral and spatial derivatives in the functional. The length scale used for the radial variable is $M_W^{-1}$. The bubble typically spreads over a range of order 100 $M_W^{-1}$. Instead of minimizing simultaneously $2N$ points describing the $h_1$ and $h_2$ profiles on the lattice, we will use an iteration method. First, to have an estimate of the bubble size, we solve a reduced problem. Assuming that the tunneling takes place along the direction given by constant $\tan\beta(T)$, we can use the standard overshooting-undershooting method to find numerically this configuration. This provides us with a good estimate of the size of the

[2] This kind of functionals has also been used to obtain unstable solutions, such as sphalerons, on the lattice [32].

lattice, where to solve the discretized problem, and also a first starting configuration for the minimization. Now, we fix one of the Higgses, $h_1$ for example, to the previous estimate and allow the $N$ points describing the other Higgs to change, minimizing the functional given in (2.10). We iterate this procedure, now fixing the $h_2$ field. We have used $N = 140$ for the discretization. In the range of the supersymmetric parameters we have explored, we found a good convergence after two or three iterations in $h_1, h_2$. Various tests derived from the fact that the obtained solutions are extremals of the Euclidean action, as e.g. the virial theorem, have been proved numerically to hold. We have also verified stability of the profiles against increasing values of $N$.

# 3 Numerical results

The strength of the phase transition, after introduction of the leading two-loop thermal corrections, has been studied in Refs. [25]-[28]. The light stop scenario was carefully analyzed in Ref. [28] where the effective potential along both the Higgs and $\widetilde{t}_R$ directions was considered, including the corresponding two-loop corrections. There, the different possibilities according to the cosmological evolution of the fields were classified as regions of stability, metastability and instability of the Higgs minimum, and regions where a two-step phase transition can proceed. In this paper we concentrate specifically in the stability region, since the metastability and two-step regions would require considering the tunneling to (and from) the color breaking minimum [33], which is outside the scope of the present paper. We will closely follow the allowed parameter space found in Ref. [28].

We choose $m_Q = 1$ TeV in such a way that the supersymmetric corrections to the $\rho$-parameter become small, giving hence a good fit to the electroweak precision data coming from LEP and SLC. On the other hand we will take as reference point $\widetilde{A}_t \equiv A_t - \mu/\tan\beta = 0$, $m_{\widetilde{t}} = 150$ GeV and $\tan\beta = 2.5$, $m_A = 200$ GeV, providing $m_h = 80$ GeV, which is consistent with present experimental bounds on the MSSM lightest Higgs mass. This particular point in the plane $(m_h, m_{\widetilde{t}})$ is acceptable from the point of view of avoiding the wipe off of the baryon asymmetry after the phase transition, as was shown in Figs. 1 and 2 of Ref. [28]. We have checked that the obtained results are rather generic, as we will explicitly show by varying the parameter $m_A$, so for other points in the allowed region of the plane $(m_h, m_{\widetilde{t}})$ we obtain similar features.

In Fig. 1 we plot the euclidean action $S_3$ (2.7) for the bounce solution (2.8) as a function of the temperature for $\widetilde{A}_t = 0$, $m_{\widetilde{t}} = 150$ GeV, $\tan\beta = 2.5$ and $m_A = 200$

GeV. We can see from Fig. 1 that $S_3$ goes to infinity at the degeneracy temperature $T_d \sim 96$ GeV, while it goes to zero at the destabilization temperature $T_0 \sim 93$ GeV. So all the phase transition happens in the 3 GeV interval shown in Fig. 1. Using that $S_3(T_c)/T_c \sim 140 - 145$ one can easily compute the value of the temperature $T_c$ [3]. For the case considered in Fig. 1 we obtain $T_c \simeq 95.2$ GeV. The corresponding profiles for the Higgs bubbles $h_1(r)$ and $h_2(r)$ are plotted in Figs. 2 and 3 [where $\rho^2(r) \equiv h_1^2(r) + h_2^2(r)$ and $\tan\beta(r) = h_2(r)/h_1(r)$, $\Delta\beta(r) = \beta(r) - \beta(T)$, $\beta(T)$ being defined by $\beta(T) \equiv v_2(T)/v_1(T)$], for $T = T_c$ (solid lines), $T = T_c + 0.4$ GeV (long-dashed lines) and $T = T_c - 0.4$ GeV (short-dashed lines).

The variation of the bubble parameters with respect to $m_A$ is displayed in Figs. 4, 5 and 6. In Fig. 4 the profile $\rho(r)/v(T_c)$ is plotted for $m_A = 100$, 200, 300 and 400 GeV, thick-solid, long-dashed, short-dashed and thin-solid curves, respectively. In all cases the bubbles have thick walls, the wall thickness being

$$L_\omega \sim (20 - 30)/T_c$$

as can be seen from Fig. 4. We can also see that wall profiles are almost indistinguisable for $m_A \gtrsim 200$ GeV. In Fig. 5 we plot the parameter $\Delta\beta \equiv \Delta\beta(\infty) - \Delta\beta(0)$ as a function of $m_A$ for the whole effective potential, including the two-loop thermal corrections (solid line) and excluding them -i.e. including only the one-loop thermal corrections- (dashed line). We see there is an enhancement due to the two-loop corrections which goes from $\sim 5$ for $m_A \sim 100$ GeV, to $\sim 2$ for $m_A \sim 400$ GeV. Since the total amount of produced baryon asymmetry is proportional to $\Delta\beta$, the latter enhancement translates into a baryogenesis enhancement, which was disregarded in previous analyses [28]. Furthermore, the enhancement produced in the strength of the phase transition, $v(T)/T$, by the two-loop thermal corrections [25]-[28] also affects the amount of baryon asymmetry produced, since the latter is proportional to [10] the integral

$$I = \int_0^\infty dr\, \frac{\rho^2(r)}{T^2}\, \frac{d\beta(r)}{dr}\ , \tag{3.1}$$

[3] The actual temperature $T_c$ at which the transition happens is readily computed by comparing the probability of bubble nucleation per unit time and unit volume, $\sim T^4 \exp\{-S_3(T)/T\}$, with the expansion rate of the universe at the corresponding temperature, $\tau^{-1} = \zeta^{-1}\ T^2/M_{\rm Pl}$, with $\zeta^{-1} = 4\pi\sqrt{\pi\left[g_B(T) + 7/8\ g_F(T)\right]/45}$. By imposing the condition that the probability for a single bubble to be nucleated within one horizon volume is $\mathcal{O}(1)$ one can compute the temperature $T_c$, i.e. from

$$\int_{T_c}^\infty \frac{dT}{T} \left(\frac{2\zeta M_{\rm Pl}}{T}\right)^4 \exp\{-S_3(T)/T\} = \mathcal{O}(1)\ .$$

and therefore the two-loop enhancement is further strengthened. In Fig. 6 we plot the integral (3.1) as a function of $m_A$, when the two-loop thermal corrections are included (solid line) and excluded (dashed line). In all cases the total enhancement is greater than one order of magnitude.

# 4 Squark bubbles

In the previous analysis we have assumed that the bubble is built by the neutral field Higgses. This ansatz, used in the Euler-Lagrange equations, is obviously consistent. However, if we want to interpret this solution as the one controlling the tunneling process, we have to analyze the variation of the Euclidean action under generic quadratic perturbations including the rest of the fields. In particular, we have to make sure that there is just one negative mode: the breathing mode.

The main candidate for such a new negative mode is provided by squark fields, in particular stop fields. If we include these field in our analysis, then the finite temperature effective potential will be now a function of four fields, $V_{eff}(h_1, h_2, \tilde{t}_L, \tilde{t}_R)$. In general, there will be directions involving the new fields $\tilde{t}_L, \tilde{t}_R$ where the potential decreases [4]. Since the kinetic term is always positive, negative modes imply necessarily negative values for the variation of the potential energy. In the quadratic approximation, this variation is given by

$$\delta^2 V_{\widetilde{t}} = 4\pi \int r^2 dr \left[ \begin{array}{cc} \widetilde{t}_L^*(r) & \widetilde{t}_R^*(r) \end{array} \right] \mathcal{M}^2_{\widetilde{t}} \left[ \begin{array}{c} \widetilde{t}_L(r) \\ \widetilde{t}_R(r) \end{array} \right] \tag{4.1}$$

where

$$\mathcal{M}^2_{\widetilde{t}}\,(h_1, h_2) = \left[ \begin{array}{cc} m_Q^2 + \Pi_{\widetilde{t}_L} + h_t^2\, h_2^2(r) & A_t\; h_t\, h_2(r) - \mu\; h_t\, h_1(r) \\ \\ A_t\; h_t\, h_2(r) - \mu\; h_t\, h_1(r) & m_U^2 + \Pi_{\widetilde{t}_R} + h_t^2\, h_2^2(r) \end{array} \right] \tag{4.2}$$

and $\Pi_{\widetilde{t}_{L,R}}$ stand for the leading $T-$dependent self-energy contributions to the thermal masses. They are proportional to $T^2$ [19, 34]. The eigenvalues of $\mathcal{M}^2_{\widetilde{t}}\,(h_1, h_2)$ give us the *masses* of the stop squarks in the Higgs background. We have to evaluate this masses along the path in the $(h_1, h_2)$ plane described by the bubble when $r$ changes from zero to infinity. Since the variation of $\tan\beta$ along this path is less than $O(10^{-2})$, we will assume that $\widetilde{A}_t$ is constant. Notice that these masses must be positive at the false and at the true vacuum because these are a local and a global minimum, respectively.

[4] This is certainly the case for some values of the parameters where new minima do appear.

These conditions translate into:

$$\begin{aligned} m_Q^2 + \Pi_{\widetilde{t}_L} &> 0 \\ m_U^2 + \Pi_{\widetilde{t}_R} &> 0 \\ (m_Q^2 + \Pi_{\widetilde{t}_L} + m_t^2)(m_U^2 + \Pi_{\widetilde{t}_R} + m_t^2) &> \widetilde{A}_t^2\, m_t^2 \end{aligned} \tag{4.3}$$

On the other hand, a necessary condition for having negative masses along the path followed by the bubble is:

$$\widetilde{A}_t^2 > m_Q^2 + \Pi_{\widetilde{t}_L} + m_U^2 + \Pi_{\widetilde{t}_R} \tag{4.4}$$

However, this condition is forbidden by the requirement of not wipping off, after the phase transition, any previously generated baryon asymmetry [28], and is never satisfied in our choice of parameter space. We then conclude that the bubble solution obtained in section 2 is not disturbed by non trivial configurations for the fields $\widetilde{t}_L$ and/or $\widetilde{t}_R$, and our conclusions in section 3 are rather robust. Had we chosen a value of the mixing $\widetilde{A}_t^2$ satisfying condition (4.4) we could have in the bubble wall a field configuration with non-trivial values of $\widetilde{t}_R$ and/or $\widetilde{t}_L$ explicitly violating baryon number.

# 5 Conclusions

In this paper we have computed the tunneling processes from the symmetric phase to the true minimum in the first order phase transition of the Higgs fields in the MSSM. We have obtained the corresponding Higgs profiles along the bubbles. We paid particular attention to the so-called light stop scenario, where the phase transition is strong enough not to wipe off any previously generated baryon asymmetry. Baryogenesis in the MSSM was previously proved to be controlled by some bubble parameters, and in particular by the integral (3.1), which were estimated by some energetic considerations based on the one-loop effective potential. We have shown, using our numerical calculations based on the two-loop effective potential, that there are important enhancement effects, with respect to those estimates, that can be around one order of magnitude. Finally we have proved that, for the considered cases, our solution is not disturbed by any non-trivial configurations of the stop fields.

## Acknowledgements

We thank D. Oaknin for useful comments and for participating in the early stages of this work.

# References


[1] A.D. Sakharov, *JETP Lett.* **91B** (1967) 24

[2] M. Shaposhnikov, *JETP Lett.* 44 (1986) 465; *Nucl. Phys.* **B287** (1987) 757 and **B299** (1988) 797. P. Arnold and L. McLerran, *Phys. Rev.* **D36** (1987) 581; and **D37** (1988) 1020; S.Yu Khlebnikov and M.E. Shaposhnikov, *Nucl. Phys.* **B308** (1988) 885; F.R. Klinkhamer and N.S. Manton, *Phys. Rev.* **D30** (1984) 2212; B. Kastening, R.D. Peccei and X. Zhang, *Phys. Lett.* **B266** (1991) 413; L. Carson, Xu Li, L. McLerran and R.-T. Wang, *Phys. Rev.* **D42** (1990) 2127; M. Dine, P. Huet and R. Singleton Jr., *Nucl. Phys.* **B375** (1992) 625

[3] For recent reviews, see: A.G. Cohen, D.B. Kaplan and A.E. Nelson, *Annu. Rev. Nucl. Part. Sci.* **43** (1993) 27; M. Quirós, *Helv. Phys. Acta* **67** (1994) 451; V.A. Rubakov and M.E. Shaposhnikov, *Phys. Usp.* **39** (1996) 461-502 [hep-ph/9603208]

[4] G.W. Anderson and L.J. Hall, *Phys. Rev.* **D45** (1992) 2685.

[5] M.E. Carrington, *Phys. Rev.* **D45** (1992) 2933; M. Dine, R.G. Leigh, P. Huet, A. Linde and D. Linde, *Phys. Lett.* **B283** (1992) 319; *Phys. Rev.* **D46** (1992) 550; P. Arnold, *Phys. Rev.* **D46** (1992) 2628; J.R. Espinosa, M. Quirós and F. Zwirner, *Phys. Lett.* **B314** (1993) 206; W. Buchmüller, Z. Fodor, T. Helbig and D. Walliser, *Ann. Phys.* **234** (1994) 260

[6] J. Bagnasco and M. Dine, *Phys. Lett.* **B303** (1993) 308; P. Arnold and O. Espinosa, *Phys. Rev.* **D47** (1993) 3546; Z. Fodor and A. Hebecker, *Nucl. Phys.* **B432** (1994) 127

[7] K. Kajantie, K. Rummukainen and M.E. Shaposhnikov, *Nucl. Phys.* **B407** (1993) 356; Z. Fodor, J. Hein, K. Jansen, A. Jaster and I. Montvay, *Nucl. Phys.* **B439** (1995) 147; K. Kajantie, M. Laine, K. Rummukainen and M.E. Shaposhnikov, *Nucl. Phys.* **B466** (1996) 189; K. Jansen, *Nucl. Phys. (Proc. Supl.)* **B47** (1996) 196; K. Rummukainen, *Nucl. Phys. (Proc. Supl.)* **B53** (1997) 30

[8] G.R. Farrar and M.E. Shaposhnikov, *Phys. Rev. Lett.* **70** (1993) 2833 and (**E**): **71** (1993) 210; M.B. Gavela. P. Hernández, J. Orloff, O. Pène and C. Quimbay, *Mod. Phys. Lett.* **9** (1994) 795; *Nucl. Phys.* **B430** (1994) 382; P. Huet and E. Sather, *Phys. Rev.* **D51** (1995) 379

[9] M. Dine, P. Huet, R. Singleton Jr. and L. Susskind, *Phys. Lett.* **B257** (1991) 351; A. Cohen and A.E. Nelson, *Phys. Lett.* **B297** (1992) 111; P. Huet and A.E. Nelson, *Phys. Lett.* **B355** (1995) 229; *Phys. Rev.* **D53** (1996)

[10] M. Carena, M. Quiros, A. Riotto, I. Vilja and C.E.M. Wagner, *Nucl. Phys.* **B503** (1997) 387

[11] J. Cline, M. Joyce and K. Kainulainen, preprint MCGILL-97-26, [hep-ph/9708393]

[12] T. Multamaki, I. Vilja, *Phys. Lett.* **B411** (1997) 301

[13] A. Riotto, preprint OUTP-97-43-P, [hep-ph/9709286]

[14] M. Worah, *Phys. Rev.* **D56** (1997) 2010

[15] M. Carena and C.E.M. Wagner, preprint FERMILAB-PUB-97-095-T, [hep-ph/9704347], to appear in 'Perspectives on Higgs Physics II', ed. G. Kane, World Scientific, Singapore, 1997

[16] H. Davoudiasl, K. Rajagopal and E. Westphal, preprint CALT-68-2127 [hep-ph/9707540]

[17] G.F. Giudice, *Phys. Rev.* **D45** (1992) 3177; S. Myint, *Phys. Lett.* **B287** (1992) 325

[18] J.R. Espinosa, M. Quirós and F. Zwirner, *Phys. Lett.* **B307** (1993) 106

[19] A. Brignole, J.R. Espinosa, M. Quirós and F. Zwirner, *Phys. Lett.* **B324** (1994) 181

[20] M. Carena, M. Quirós and C.E.M. Wagner, *Phys. Lett.* **B380** (1996) 81

[21] D. Delepine, J.M. Gérard, R. González Felipe and J. Weyers, *Phys. Lett.* **B386** (1996) 183

[22] J.M. Moreno, D.H. Oaknin and M. Quirós, *Nucl. Phys.* **B483** (1997) 267; *Phys. Lett.* **B395** (1997) 234

[23] J. Cline and K. Kainulainen, *Nucl. Phys.* **B482** (1996) 73; preprint MCGILL-97-7, [hep-ph/9705201]

[24] M. Laine, *Nucl. Phys.* **B481** (1996) 43; M. Losada, *Phys. Rev.* **D56** (1997) 2893; preprint [hep-ph/9612337]; G. Farrar and M. Losada, *Phys. Lett.* **B406** (1997) 60

[25] J.R. Espinosa, *Nucl. Phys.* **B475** (1996) 273

[26] B. de Carlos and J.R. Espinosa, *Nucl. Phys.* **B503** (1997) 24

[27] D. Bodeker, P. John, M. Laine and M.G. Schmidt, *Nucl. Phys.* **B497** (1997) 387

[28] M. Carena, M. Quiros and C.E.M. Wagner, preprint FNAL-Pub-97/327-T, CERN-TH/97-190, IEM-FT-165/97 [hep-ph/9710401]

[29] Y. Brihaye and J. Kunz *Phys. Rev.* **D48** (1993) 3884.

[30] S. Coleman, V. Glaser and A. Martin, *Commun. Math. Phys.* **58** (1978) 211

[31] A. Kusenko, *Phys. Lett.* **B358** (1995) 51

[32] M. García-Pérez and P. van Baal, *Nucl. Phys.* **B468** (1996) 277

[33] J.M. Moreno, M. Quirós and M. Seco, in preparation

[34] D. Comelli and J.R. Espinosa, *Phys. Rev.* **D55** (1997) 6253

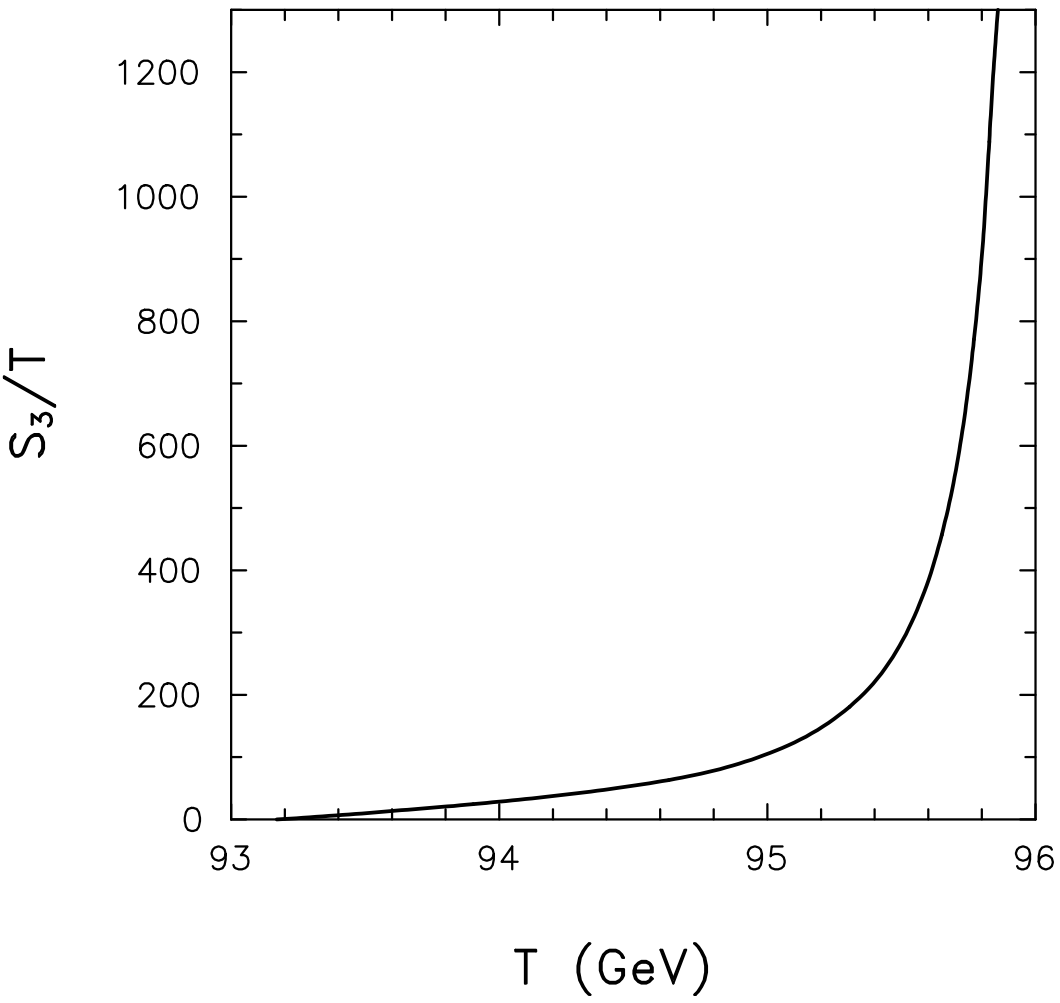


Figure 1: The Euclidean action as a function of the temperature for $m_Q = 1$ TeV, $\tan\beta = 2.5$, $\widetilde{A}_t = 0$, $m_{\widetilde{t}} = 150$ GeV, and $m_A = 200$ GeV.

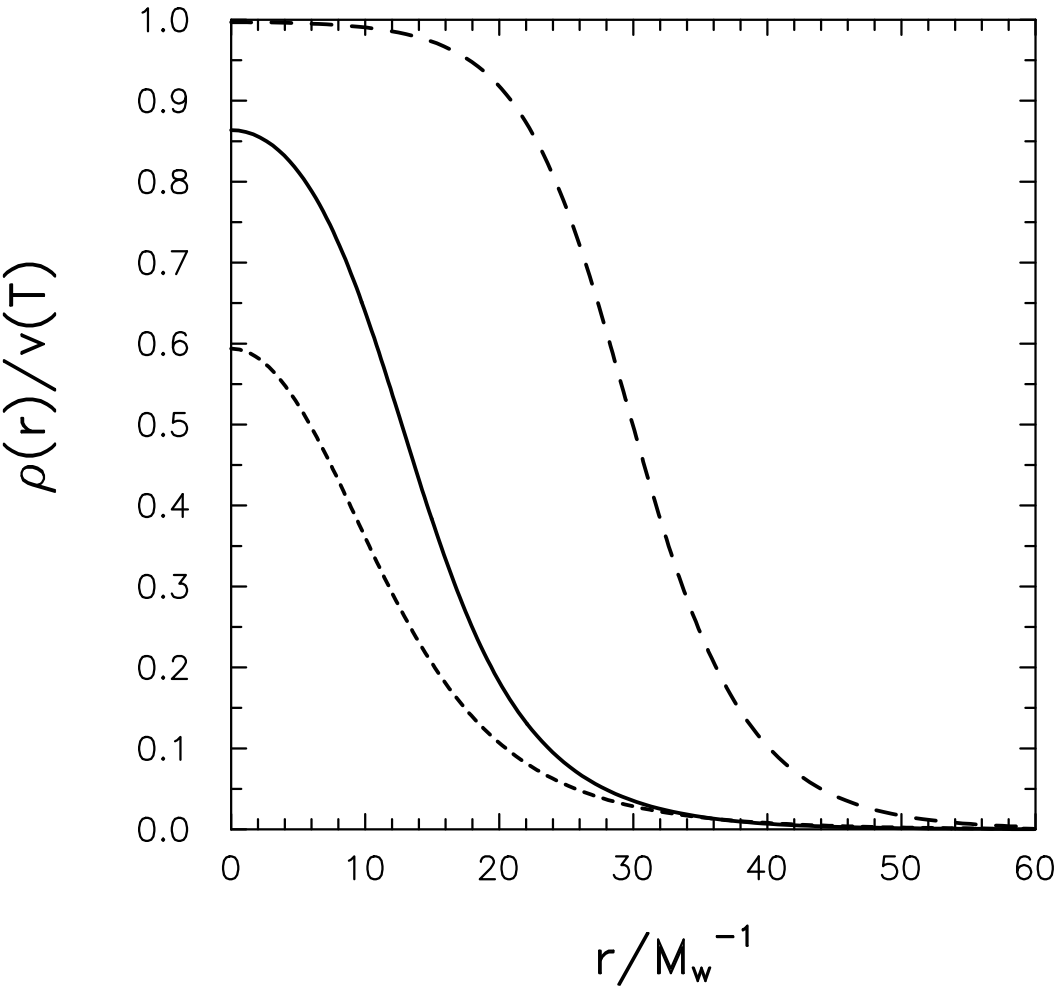


Figure 2: The Higgs profile $\rho(r)/v(T)$ for $T = T_c + 0.4$ GeV (long-dashed curve) and $T = T_c - 0.4$ GeV (short-dashed curve), and values of supersymmetric parameters as in Fig. 1.

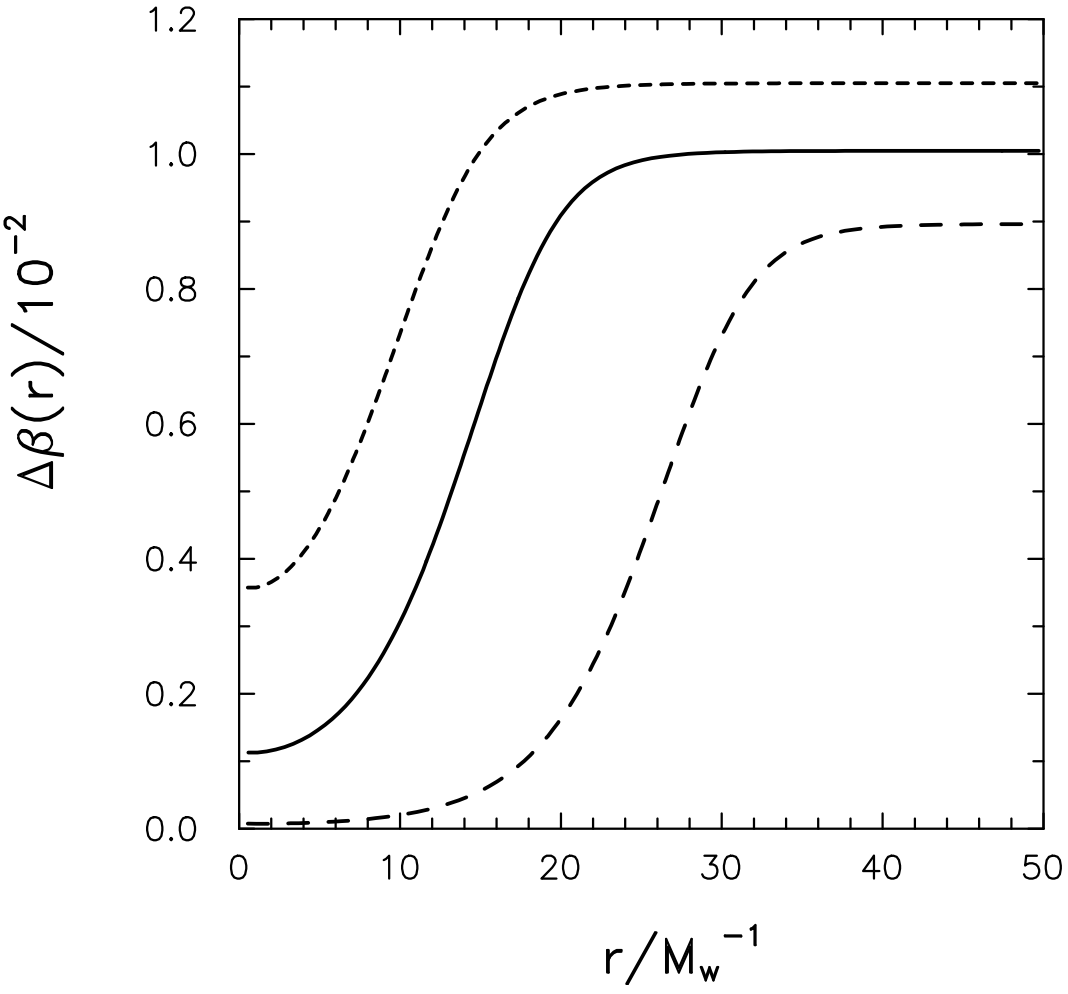


Figure 3: The same as in Fig. 2 but for the Higgs profile $\Delta\beta(r)$.

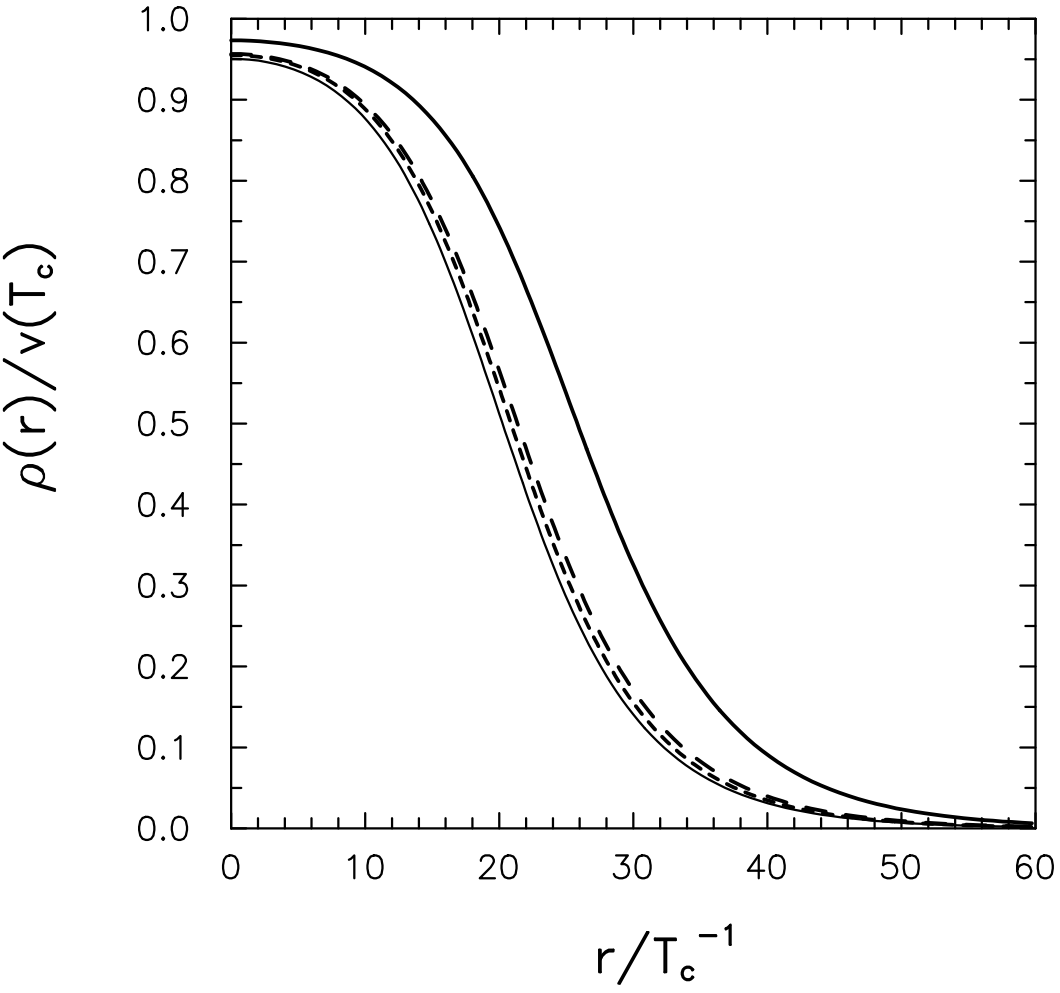


Figure 4: Higgs profile $\rho(r)/v(T_c)$ for $m_Q = 1$ TeV, $\tan\beta = 2.5$, $\widetilde{A}_t = 0$, $m_{\widetilde{t}} = 150$ GeV, and $m_A = 100$ GeV (thick-solid curve), 200 GeV (long-dashed curve), 300 GeV (short-dashed curve) and 400 GeV (thin-solid curve).

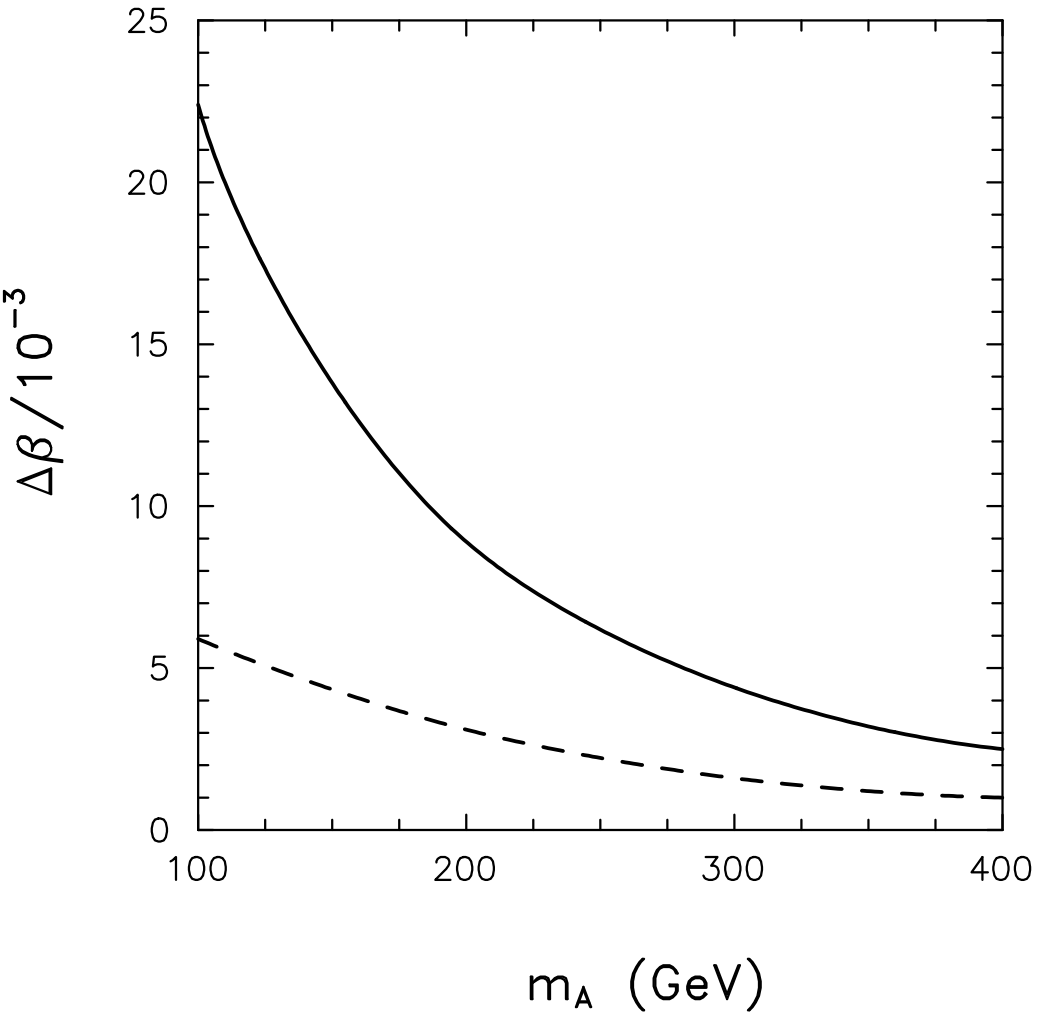


Figure 5: The parameter $\Delta\beta$ in the two-loop (solid curve) and one-loop (dashed curve) approximations, for $m_Q = 1$ TeV, $\tan\beta = 2.5$, $\widetilde{A}_t = 0$ and $m_{\widetilde{t}} = 150$ GeV, as a function of $m_A$.

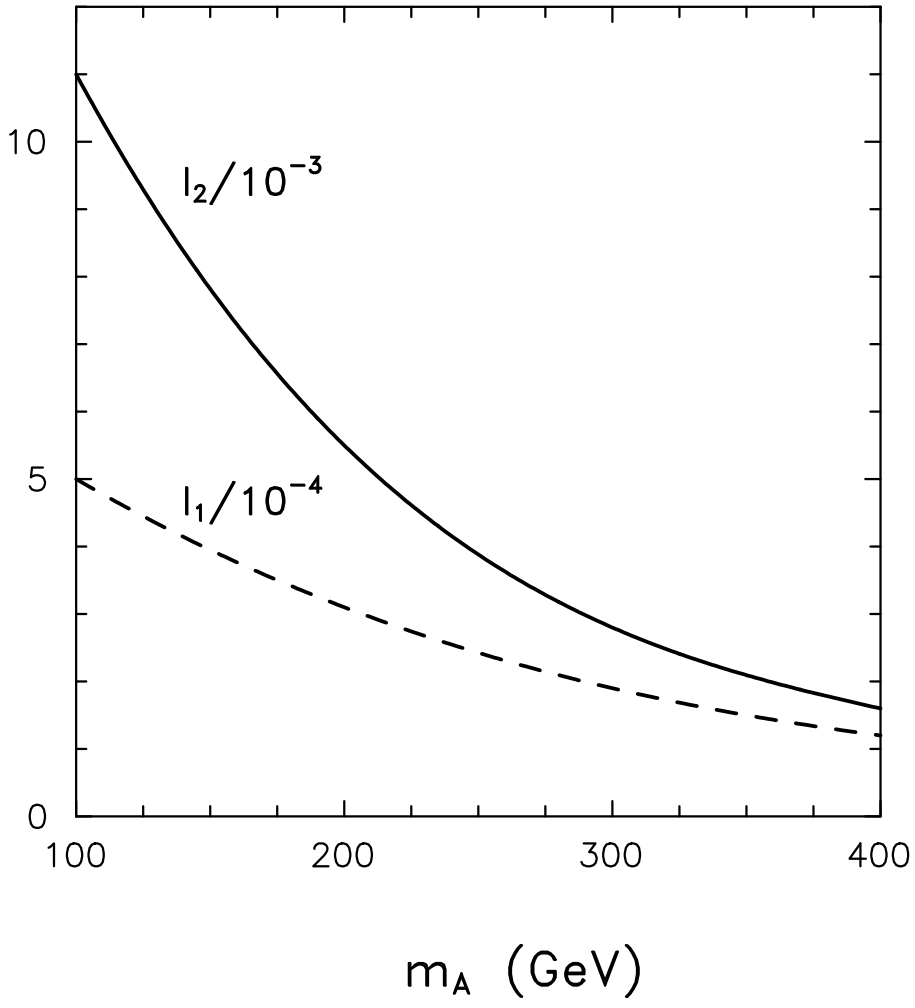


Figure 6: The same as in Fig. 5 but for the integral $I_\ell$ (3.1), $\ell$=1-loop (dashed curve), $\ell$=2-loop (solid curve).